Original Article

miR-145-5p targets MMP2 to protect brain injury in hypertensive intracerebral hemorrhage via inactivation of the Wnt/β-catenin signaling pathway

Wenfeng Xiao[1,2], Zhengfang Jiang[2], Weifeng Wan[3], Wen Pan[4], Jianguo Xu[1]

[1]Department of Neurosurgery, West China Hospital, Sichuan University, Chengdu, China; [2]Department of Neurosurgery, Sichuan Mianyang 404 Hospital, Mianyang, China; [3]Department of Neurosurgery, Southwest Medical University, Luzhou, China; [4]Department of Neurosurgery, Shougang Shuigang General Hospital, Liupanshan, China

Contributions: (I) Conception and design: W Xiao; (II) Administrative support: J Xu; (III) Provision of study materials or patients: W Xiao, Z Jiang; (IV) Collection and assembly of data: W Xiao, W Wan; (V) Data analysis and interpretation: W Xiao, W Pan; (VI) Manuscript writing: All authors; (VII) Final approval of manuscript: All authors.

Correspondence to: Jianguo Xu. Department of Neurosurgery, West China Hospital, Sichuan University, Guoxue Street 37, Chengdu 610041, China. Email: xujg@scu.edu.cn.

Background: Differences in microRNA (miRNA) expression after hypertensive intracerebral hemorrhage (HICH) have been reported in human and animal models. miRNA-145 plays an important role in vascular endothelial cells. The purpose of this work was to determine the role of miR-145-5p in HICH and the molecular mechanisms by which it acts.

Methods: In this study, we constructed a model of hemoglobin-induced HICH in rats and used thrombin-treated human brain microvascular endothelial cells (hBMECs) to create a HICH cell model. To determine brain damage, we tested the rats' neurological performance and measured the cerebral water level of their brain tissue. Cell counting kit 8 (CCK8) was used to determine the viability of cells. Apoptosis was detected using the terminal TdT-mediated dUTP nick end labeling (TUNEL) assay and flow cytometry (FCM). Starbase and TargetScan were used to predict and confirm target genes. Luciferase reporter gene experiments were used to confirm the predictions. Reverse transcription-polymerase chain reaction (RT-PCR) and Western blotting were used to identify the associated genes and proteins.

Results: We observed a reduction in miRNA-145-5p expression in both the HICH cell model and the rat model. miRNA-145-5p overexpression increased cell survival and preserved newly created blood vessels and vascular permeability in hBMECs. MiRNA-145-5p has been predicted to target matrix metalloproteinase 2 (MMP2). Additionally, MMP2 was identified as a miR-145-5p target gene and shown to be substantially expressed in the thrombin-treated hBMECs. MMP2 overexpression suppressed miR-145-5p-mediated effects and increased hBMECs' malfunction. In comparison with controls, the HICH + AAV-miR-145-5p group performed better on behavioral tests and had less brain water. Additionally, miR-145-5p injection increased ZO-1 and occludin expressions, as determined by immunohistochemical staining in the HICH rat model.

Conclusions: miRNA-145-5p protects against brain injury following HICH by targeting MMP2, suggesting a possible therapeutic mechanism for HICH.

Keywords: Human brain microvascular endothelial cells (hBMECs); hypertensive intracerebral hemorrhage (HICH); miRNA-145-5p; matrix metalloproteinase 2 (MMP2)

Submitted Mar 01, 2022. Accepted for publication May 17, 2022.
doi: 10.21037/atm-22-1897
View this article at: https://dx.doi.org/10.21037/atm-22-1897

Introduction

The complications of hypertension can be disabling. Intracranial hemorrhage (ICH) is most frequently caused by hypertension (1). ICH-induced brain injury leads to irreversible disruption of the blood-brain barrier (BBB) and fatality brain edema with massive cell death (2). Specifically, hypertensive intracerebral hemorrhage (HICH) is a common complication of neurosurgery and is frequently seen in hypertensive patients (1,3,4). The frequency of HICH continues to rise in lockstep with the aging population, with high mortality and morbidity, gravely endangering patients' lives (5). At the moment, the primary treatments for HICH are craniotomy and conservative management, but patient outcomes remain poor.

MicroRNAs (miRNAs) are a group of non-coding RNAs that are found in eukaryotes and have many different roles (6). They help the silencing complex remove the target mRNA or stop the target mRNA from being translated (7). It has already been shown that miRNAs are important for many different biological and medical processes (8). Recently, a number of miRNAs have been found to be different in people with ICH, such as miR-19b-3p (9), miR-383-3p (10), and miR-144/451 (11), which suggests that these miRNAs may play a role in the development of ICH (12). miR-145 has been widely confirmed as a phenotypic marker and modulator of contractile vascular smooth muscle cells (VSMCs) (13-16), and recent study has shown it also plays an important role in vascular endothelial cells, inhibiting angiogenesis through targeted regulation of vascular endothelial growth factor (VEGF)-A and ANGPT2 in models of injury human brain microvascular endothelial cells (hBMECs) induced by oxygen and glucose deprivation (OGD) (17). Li *et al.* (18) found that miR-145-5p alleviated the damage to cardiac microvascular endothelial cells in coronary artery disease induced by hypoxia/reoxygenation by inhibiting the expression of Smad4. However, the specific effects of miR-145-5p after HICH remain to be clarified. In our previous study, through gene chip screening, miR-145-5p showed significant differences between the hypertension group and the hypertension-related cerebral hemorrhage group, and was involved in gene regulation of multiple pathways. Matrix metalloproteinases (MMPs) are zinc-dependent, proteolytic endopeptidases involved in ICH progression. The activation of MMP-2 in chronic microbleeds and acute ICH was believed to be responsible for triggering the eventual bleeding (19). As a result, we examined the effect of miR-145-5p/MMP2 on vascular endothelial cell damage in both the HICH rat model and hBMECs in the current work. The goal of this research was to discover a novel therapy for HICH. We present the following article in accordance with the ARRIVE reporting checklist (available at https://atm.amegroups.com/article/view/10.21037/atm-22-1897/rc).

Methods

Animals and groups

Male spontaneously hypertensive rats weighing 250–300 g (aged 6–8 weeks) were purchased from SPF Biotechnology Co., Ltd. (SCXK No. 2019-0010; Beijing, China), and maintained under a 12-h light/12-h dark cycle, with standard food and water. Rats were randomly divided into 4 groups, including sham (n=10), HICH (n=10), HICH + AAV-control (n=10), HICH + AAV-miR-145-5p groups (n=10). The animal experiments were performed according to the National Institutes of Health's Guidelines for the Care and Use of Laboratory Animals and were granted approval by the Animal Care and Research Committee of West China Hospital of Sichuan University (No. 20211047A).

Establishment of HICH model

The rats were anesthetized with isoflurane and immobilized. An incision was made along the sagittal midline to expose the skull. After drilling a 1 mm hole in the skull, a syringe is inserted into the right caudate nucleus (3.4 mm outside the midline, 1 mm in front of the junction of the coronal and sagittal sutures of the skull, 6 mm below the surface of the skull) and then withdrawn 0.5 mm. Using a microinjection pump, 20 μL hemoglobin (Sigma) and 10 μL adenovirus [miR-145-5p overexpressed adenovirus or negative control adenovirus, 1×10^{10} plaque forming unit (PFU)/mL] at a concentration of 150 mg/mL were injected into the nucleus within 10 min. After injection, the needle was left in place for another 10 min to prevent reflux, then slowly removed, the hole sealed with bone wax, and the incision closed.

Behavioral testing

Modified neurological severity score (mNSS) (combined scores of motor, sensory, reflexes and balance tests) were

performed 24, 48 and 72 h after modeling, and neurological function was rated on a scale of 0–18 (normal score 0; maximum defect score 18). On a severity scale of injury, a score of 13–18 indicates serious injury, 7–12 indicates moderate injury, and 1–6 indicates mild injury.

Modified limb placing tests (mLPTs) were performed at 24, 48, and 72 h after modeling. While holding the rat by its torso, forelimbs hanging free, the vibrissae were brushed against the corner edge of a table. Non-brain damaged rats will typically place the forelimb ipsilateral to the side of vibrissae stimulation onto the table. Depending on the extent of injury, the paw placement ability of the rat will be impaired. Each rat's forelimb was tested 10 times and the percentage of rats that placed the appropriate forelimb at the edge of the table in response to vibrissae stimulation was determined.

Measurements of brain water content

The brain of animals were removed after euthanasia and fixed by immersion in 10% buffered formalin. All brain tissue samples from the ipsilateral basal ganglia were immediately weighed to obtain wet weight (Ww) and then dried in a drying oven at 100 ℃ for 48 h to obtain the dry weight (Dw). The cerebral water content was calculated as: (Ww – Dw)/Ww ×100%

Histopathological examination (HE), TdT-mediated biotinylated nick end-labeling (TUNEL) assay and immunohistochemistry (IHC)

The brain tissues were embedded into paraffin blocks and were cut at a thickness of 5 μm tissue sections. For the histopathological examination, sections were stained with hematoxylin and eosin. The TUNEL staining procedure was carried out according to the manufacturer's instructions before analysis using a light microscope and LEICA software version 2.0. The localizations of tight junction-associated proteins in HICH rat model was detected by Immunohistochemistry. For the rat brain, IHC labeling was performed using a routine method on 4-μm slices produced from paraffin-embedded tissue samples of ischemic brains. Finally, diaminobenzidine was used to visualize immunoreactivity. The following antibodies were used: anti-occludin (Proteintech, 1:200), anti-zonula occludens-1 (anti-ZO-1, Proteintech, 1:200).

Cell culture, treatment and transfection

hBMECs were purchased from iCell (iCell Bioscience Inc., Shanghai, China) and grown at 37 ℃ in a 5% CO_2 incubator in fetal bovine serum in DMEM media. hBMECs were treated with thrombin (10, 20 U/mL) for 24 h to establish ICH cell model. These cells were transfected with negative control mimics (mimics NC), miR-145-5p mimics, negative control inhibitor (inhibitor NC), miR-145-5p inhibitor using Lipofectamine 3000 following the manufactures' instructions.

Proliferation assay

The Cell Counting Kit 8 (CCK8 Kit; Beyotime Biotechnology) was used to evaluate cell viability in accordance with the manufacturer's instructions. Cells were plated in 96-well plates and seeded at a density of 1×10^4 cells/well in a full-growth medium. Using a microplate reader (BIOBASE-EL10A), the plates were evaluated after 1.5 h of incubation at 37 ℃.

Flow cytometry assay

The Annexin V-FITC Apoptosis Detection Kit (Meilunbio) was used to evaluate cell death in the hBMECs. For 1 h in the dark at room temperature, the transfected cells were incubated in 200 μL binding buffer containing 10 μL Annexin V-FITC and 5 μL propidium iodide (PI). Flow cytometry was then used to determine apoptosis. The results of the flow analysis were processed using the Flowjo software.

miRNA target prediction

MiR-145-5p target gene prediction was performed using the StarBase, miRanda and TargetScan databases.

Luciferase reporter assay

Plasmids were produced using a pmirGLO dual-luciferase miRNA expression vector (Promega, USA), MMP2 wild-type (MMP2-WT), and mutant (MMP2-MUT). Lipofectamine 3000 was used to cotransfect miR-145-5p mimics and MMP2-WT/MUT plasmids into hBMECs (Invitrogen). Finally, 48 h after transfection, luciferase

Table 1 Primer sequences for quantitative real-time PCR

RT-PCR assays	Primers	Sequences (5'-3')
GAPDH	PCR forward primer	ATGACATCAAGAAGGTGGTGAAGCAGG
	PCR reverse primer	GCGTCAAAGGTGGAGGAGTGGGT
VEGFA	PCR forward primer	GTGCCCGCTGCTGTCTAATGCC
	PCR reverse primer	GTACGTTCGTTTAACTCAAGCTGCCTC
MMP2	PCR forward primer	TGAGGACTACGACCGCGACAA
	PCR reverse primer	TGGGCTGCCACGAGGAACA
TLR4	PCR forward primer	AGGATGAGGACTGGGTAAGG
	PCR reverse primer	CTGGATGAAGTGCTGGGAC
miR-145-5p	Reverse transcription primer	GTCGTATCCAGTGCAGGGTCCGAGGTGCACTGGATACGACAGGGATT
	PCR forward primer	TGCGGGTCCAGTTTTCCCAGGAAT
	PCR reverse primer	CCAGTGCAGGGTCCGAGGT
U6	Reverse transcription primer	AACGCTTCACGAATTTGCGTG
	PCR forward primer	GCTCGCTTCGGCAGCACA
	PCR reverse primer	AACGCTTCACGAATTTGCGTG

RT-PCR, reverse transcription-polymerase chain reaction; VEGFA, vascular endothelial growth factor-A; MMP2, matrix metallopeptidase 2; TLR4, Toll-like receptor 4; GAPDH, glyceraldehyde-3-phosphate dehydrogenase.

activity was determined using a dual-luciferase reporter assay kit.

In vitro vascular permeability assay

hBMECs were inoculated in a Transwell chamber at a density of 2.5×10^4, and the original medium in the chamber was discarded and replaced with a medium containing 0.01% FITC-dextran 20K solution (Xi'an Ruixi Biotechnology). The medium in the lower chamber was collected at different time points (0, 60 and 120 min), and the fluorescence intensity was measured with a microplate analyzer (485 nm excitation, and 520 nm emission).

Tube formation assay

Matrigel was melted overnight at 4 ℃, then diluted with basal medium (DMEM) at a ratio of 1:1, before evenly spreading 50 μL in each well of 96-well plate and incubating at 37 ℃ for 30 min to solidify. The cells of different groups (control, HICH, HICH + mimics NC, HICH + miR-145-5p mimics, HICH + inhibitor NC, HICH + miR-145-5p inhibitor, HICH + miR-145-5p mimics + pcDNA3.1, HICH + miR-145-5p mimics + pcDNA3.1-MMP2) were resuspended and diluted to a 3×10^5 cells/mL suspension. Next, 100 μL of the single-cell suspension was added to the surface of the Matrigel, and incubation at 37 ℃ for 4 h. The vascular network structure was observed under a microscope and the total number of vascular loops was analyzed.

Real-time quantified PCR (RT-PCR)

Total RNA was extracted using TRIZOL reagent (Invitrogen) as directed by the manufacturer and reverse transcription reactions were performed using the PrimeScript RT reagent kit (Takara). The $2^{-\Delta\Delta Ct}$ technique was used to quantify the quantitative expression of target genes. The sequences of primer pairs are in *Table 1*.

Western blot assay

Proteins were extracted from samples (tissue and cultured cells) using RIPA buffer containing 1 mM phenylmethanesulfonyl fluoride (PMSF) (SolarBio) and separated by SDS-PAGE at 8–10%. The proteins were then transferred to a polyvinylidene fluoride membrane to be probed with Bax (Immunoway, 1:1,000), Bcl-2 (Immunoway, 1:1,000), Caspase 3 (Immunoway, 1:1,000), MMP2

(Immunoway, 1:1,000), Wnt3 (Immunoway, 1:1,000), Wnt5a (Immunoway, 1:1,000), β-catenin (Proteintech, 1:1,000), TCF-4 (Proteintech, 1:1,000), LEF-1(Proteintech, 1:1,000), IL-8 (Immunoway, 1:1,000) and GAPDH (Proteintech, 1:1,000) for 24 h at 4 ℃. Next, the proteins were incubated with appropriate secondary antibody for 2 h at approximately 25 ℃. All western blots were repeated at least 3 times. The density of the immunoreactive bands was quantified using ImageJ software.

Statistical analysis

The data are presented as mean and standard deviations and were analyzed using SPSS 10.0. Student's *t*-test or one-way analysis of variance was used to determine comparisons between groups. $P<0.05$ was used to determine if differences were significant.

Results

Attenuation of thrombin-induced injury in hBMECs by miR-145-5p overexpression

Thrombin has a critical function in the development of cerebral edema following HICH. Because thrombin stimulation of hBMECs *in vitro* results in a similar change in cell shape to that observed *in vivo* (20), we used thrombin stimulation to develop the HIHC cell model. We found that the treatment with thrombin for 24 h resulted in a distinct change in the morphology in hBMECs (*Figure 1A*). *Figure 1B* shows miR-145-5p expression downregulated by thrombin in a dose-dependent manner. Cell viability was considerably raised in the HICH + miR-145-5p mimics group when compared with the HICH + mimics NC groups, whereas cell viability was dramatically lowered in the HICH + miR-145-5p inhibitor group when compared with the HICH + inhibitor NC group in subsequent CCK8 experiment (*Figure 1C*). According to our findings, overexpression of miR-145-5p may successfully reduce thrombin-induced apoptosis in hBMECs, and silencing of miR-145-5p can substantially promote apoptosis of the same cells (*Figure 1D*,*1E*).

To further evaluate the effect of miR-145-5p in HICH, vascular permeability and tube formation assays were performed. As shown in *Figure 2A*, angiogenesis was promoted in the HICH + miR-145-5p mimics group and inhibited in the HICH + miR-145-5p inhibitor group. Moreover, as shown in *Figure 2B*,*2C*, vascular permeability in the HICH + miR-145-5p mimics group was much lower than that of cells in the HICH + mimics NC group, and silencing miR-145-5p significantly increased vascular permeability.

Regulation of hBMECs function by miR-145-5p

To get a better understanding of how miR-145-5p affects the functioning of hBMECs, a bioinformatics analysis using TargetScan, miRanda, and StarBase determined the probable miR-145-5p target genes. The miR-145-5p binding sequences for vascular endothelial growth factor (VEGFA), MMP2, and Toll-like receptor 4 (TLR4) are displayed in *Figure 3A*. Subsequently, we verified that transfection of miR-145-5p mimics substantially decreased MMP2 production, as did transfection of miR-145-5p mimics (*Figure 3B*). Additionally, the findings of the luciferase reporter gene experiment revealed that miR-145-5p may target the 3'UTR of MMP2 (*Figure 3C*). It was also found that the transfection of cells with miR-145-5p mimics decreased the protein expression of MMP2 in hBMECs (*Figure 3D*).

To explore the changes of MMP2 in HICH and the interaction between miR-145-5p and MMP2, we determined whether the expression levels of MMP2 were changed in HICH cell model. As shown in *Figure 4A*,*4B*, HICH induced a significant elevation of MMP2 mRNA and protein expression levels. Remarkably, the presence of miR-145-5p mimic significantly reversed the high expression of MMP2 caused by HICH. The Wnt/β-catenin signaling pathway has been implicated in the etiology of ICH in previous investigations (21). We also studied the changes in protein expression of the Wnt/β-catenin signaling pathway downstream target genes, such as MMP2, Wnt3, Wnt5a, β-catenin, TCF-4, LEF-1 and IL-8, using western blot assay. A noticeable decrease in the expressions of MMP2, Wnt3, β-catenin, TCF-4, LEF-1 and IL-8 was observed after overexpressing miR-145-5p, and an increase in expression was observed after inhibition of miR-145-5p (*Figure 4B*).

Effect of miR-145-5p/MMP2 axis in HICH cell model

Additionally, we conducted a rescue experiment to determine whether miR-145-5p regulates MMP2 expression in thrombin-treated hBMECs. According to the CCK-8 findings (*Figure 5A*), induction of miR-145-5p expression significantly increased cell survival among

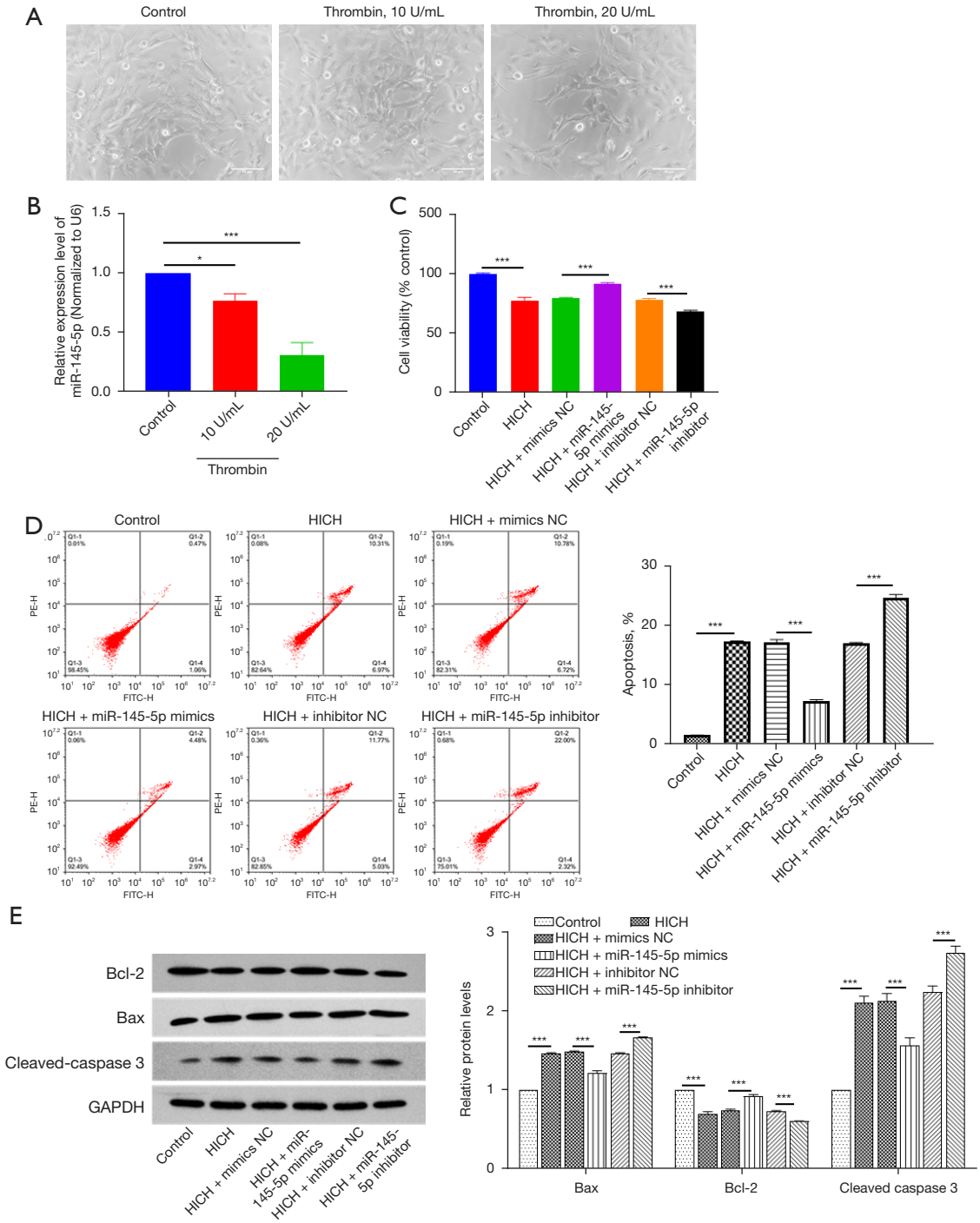

Figure 1 Effect on miR-145-5p in hBMECs after treatment with thrombin. (A) Cell morphology changes after 24 h incubation with thrombin (10, 20 U/mL) were observed by light microscopy (400× magnification, scale bar: 50 μm). (B) Cells treated with 10 and 20 U/mL of thrombin for 24 h, and relative expression of miR-145-5p measured by RT-PCR. After treatment with 20 U/mL of thrombin, along with mimics NC or miR-145-5p mimics, cell viability (C), apoptosis (D), and apoptosis-related proteins Bax, Bcl-2, and cleaved-caspase 3 (E) in hBMECs were determined by CCK-8, flow cytometry, and western blot. Data are expressed as mean ± SD. *, P<0.05; ***, P<0.001. hBMECs, human brain microvascular endothelial cells; RT-PCR, reverse transcription-polymerase chain reaction; NC, negative control; SD, standard deviation; HICH, hypertensive intracerebral hemorrhage; GAPDH, glyceraldehyde-3-phosphate dehydrogenase.

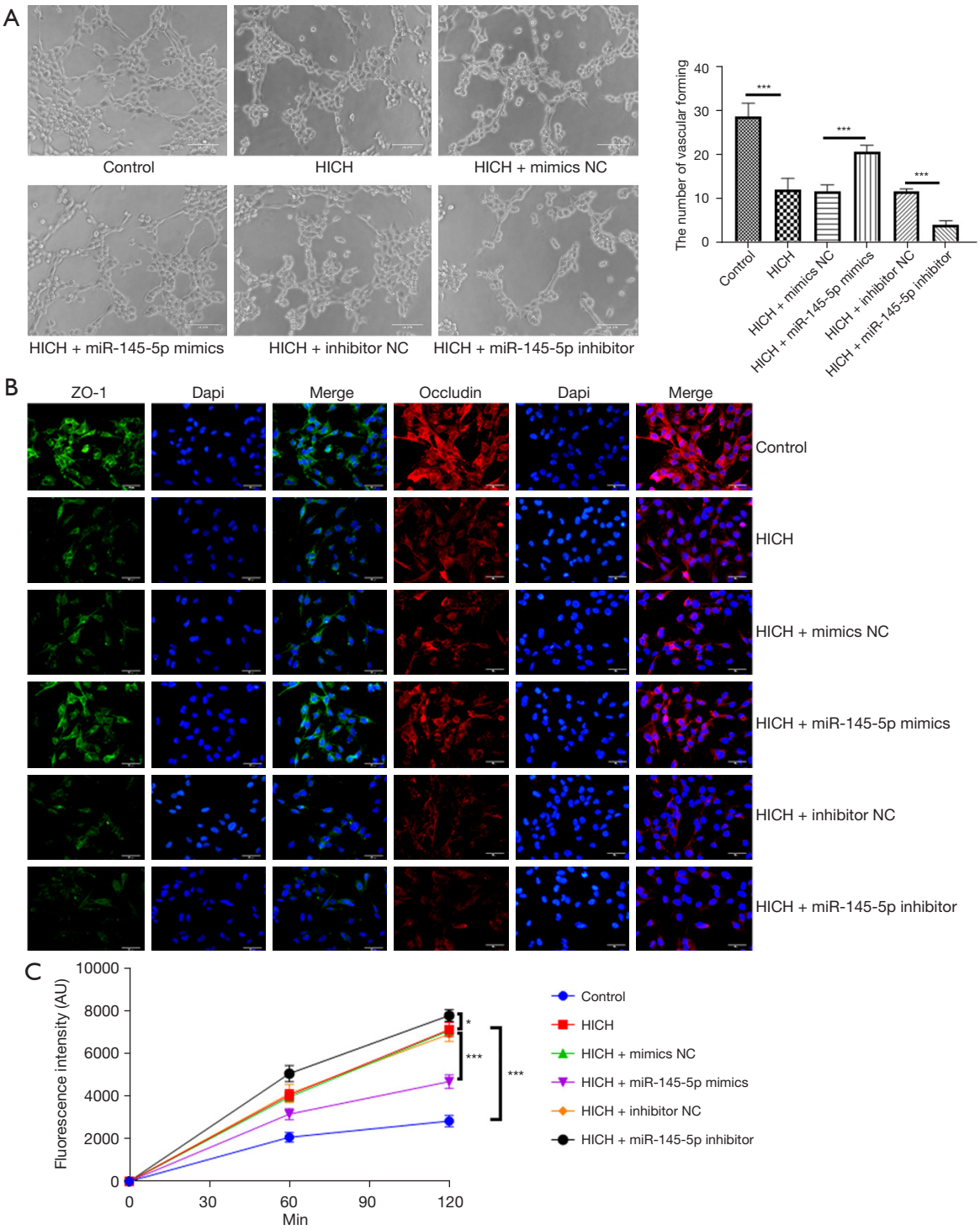

Figure 2 Effect of miR-145-5p on thrombin-treated hBMECs. (A) Representative images showing changes in the capillary-like structure of hBMECs observed by Matrigel tube formation assay under different conditions (200× magnification, scale bar: 50 μm). (B) Distribution and expression of tight junction-related proteins were detected by immunofluorescence assay (400× magnification, scale bar: 50 μm). (C) After FITC-dextran was added, fluorescence intensity (AU) over time were quantified as a reflection of alterations in vascular permeability. Results are presented as mean ± SD and *, P<0.05; ***, P<0.001. hBMECs, human brain microvascular endothelial cells; HICH, hypertensive intracerebral hemorrhage; FITC, fluorescein isothiocyanate; NC, negative control; AU, arbitrary unit.

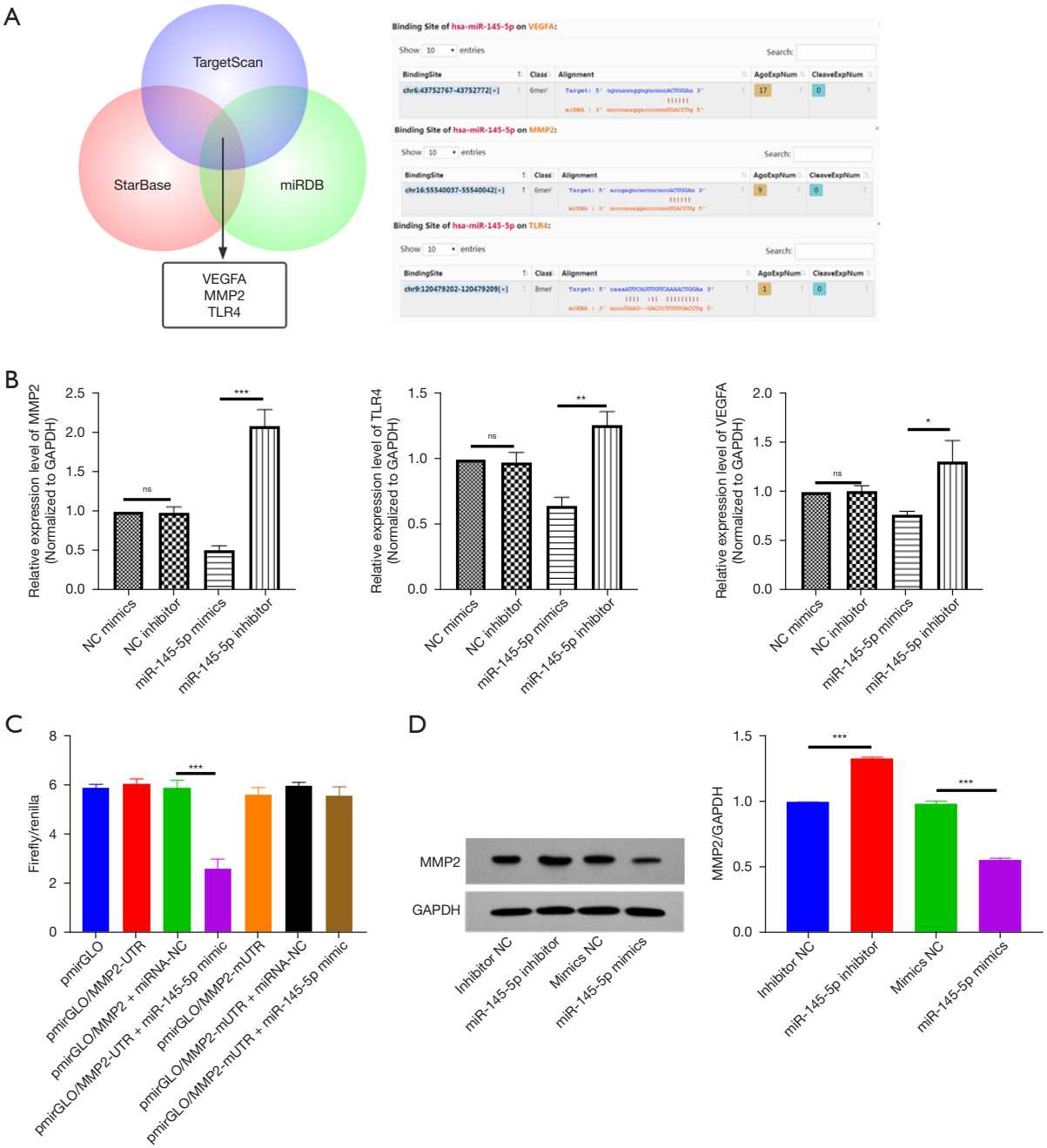

Figure 3 Binding of miR-145-5p to MMP2. (A) miRNAs bound to MMP2 were analyzed using miRDB, StarBase and TargetScan. Predicted binding sites between MMP2 and miR-145-5p. (B) MMP2, VEGFA and TLR4, were measured using RT-PCR. (C) Luciferase reporter assay was conducted to detect luciferase activity. (D) Expression of MMP2 was detected by western blot. Results are presented as mean ± SD. NS, no significance; *, P<0.05; **, P<0.01; ***, P<0.001. MMP2, matrix metallopeptidase 2; VEGFA, vascular endothelial growth factor-A; TLR4, Toll-like receptor 4; RT-PCR, reverse transcription-polymerase chain reaction; SD, standard deviation; GAPDH, glyceraldehyde-3-phosphate dehydrogenase; NC, negative control.

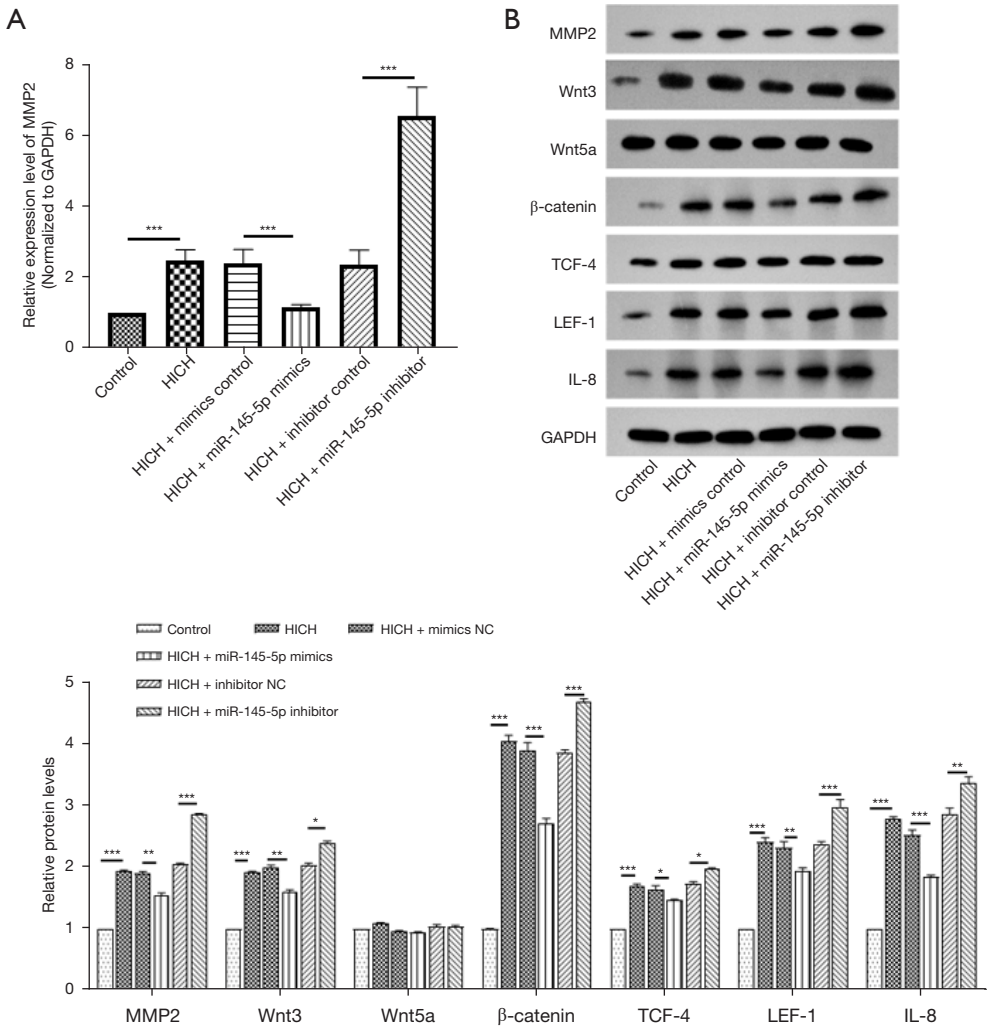

Figure 4 Effect of overexpression of miR-145-5p on the Wnt/β-catenin signaling pathway in thrombin-treated hBMECs. (A) Changes in mRNA expression of MMP2; (B) protein levels of MMP2, Wnt3, Wnt5a, β-catenin, TCF-4, LEF-1 and IL-8 in different groups detected by RT-PCR and western blot analysis, respectively. Results are presented as mean ± SD. *, P<0.05; **, P<0.01; ***, P<0.001. hBMECs, human brain microvascular endothelial cells; RT-PCR, reverse transcription-polymerase chain reaction; NC, negative control; SD, standard deviation; HICH, hypertensive intracerebral hemorrhage; GAPDH, glyceraldehyde-3-phosphate dehydrogenase; MMP2, matrix metallopeptidase 2; TCF-4, transcription factor 4; LEF-1, lymphoid enhancer binding factor 1; IL-8, interleukin-8.

thrombin-treated hBMECs compared with control cells, and overexpression of MMP2 reversed this effect. We observed that overexpression of miR-145-5p in thrombin-treated hBMECs significantly decreased the number of apoptotic cells compared with the HICH group, whereas cotransfection with miR-145-5p mimic and pcDNA3.1-MMP2 significantly increased the number of apoptotic cells compared with the miR-145-5p mimic group (*Figure 5B*). Additionally, the effect of the miR-145-5p/MMP2 axis on apoptotic proteins was determined using a western blot experiment (*Figure 5C*). As shown in *Figure 5D*, the overexpression of MMP2 partly reversed the increased ability of miR-145-5p overexpression on tube formation. Moreover, MMP2 overexpression distinctly reversed the inhibiting actions of miR-145-5p overexpression on vascular permeability (*Figure 5E*) by suppressing the expression of ZO-1 and occludin (*Figure 5F*). Western blot showed that Wnt and β-catenin proteins in hBMECs were downregulated via miR-145-5p mimics, but reversed by MMP2 overexpression (*Figure 5G*).

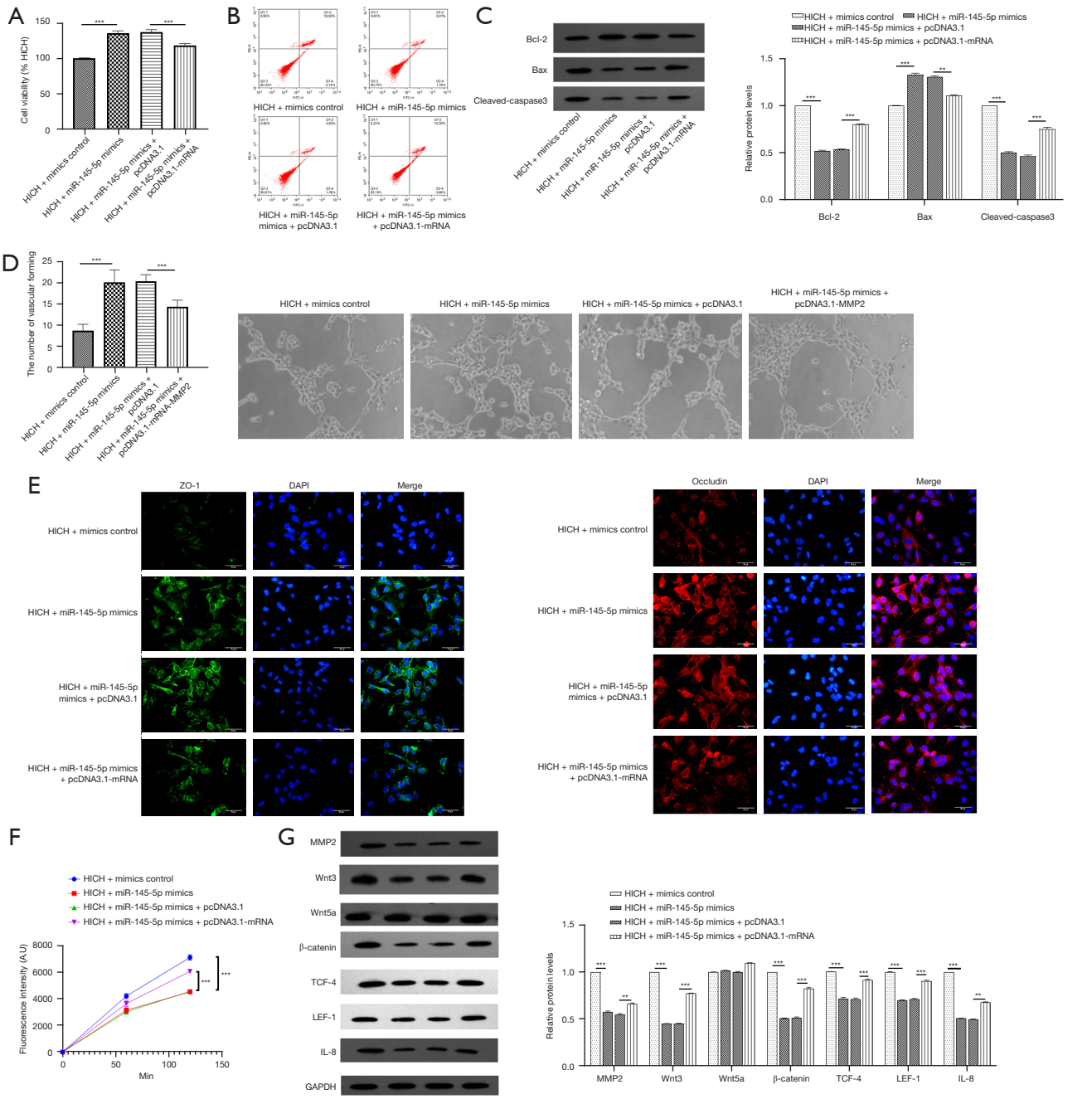

Figure 5 Effect of miR-145-5p/MMP2 axis on the biological behavior of thrombin-treated hBMECs. (A) CCK8 assay of the proliferation of transfected hBMECs in each group; (B) flow cytometry to detect apoptosis of hBMECs in each group; (C) apoptosis-related proteins Bax, Bcl-2, and cleaved-caspase 3 determined by Western blot; (D) matrigel assay was used to assess the formation of capillary-like structures in hBMECs (400× magnification); (E) expression of ZO-1 and occludin was determined by immunofluorescence (400× magnification, scale bar: 50 μm); (F) vascular permeability was evaluated using FITC-labeled dextran. (G) Protein expression levels of MMP2, Wnt3, Wnt5a, β-catenin, TCF-4, LEF-1 and IL-8 in the 4 experimental groups. Results are presented as mean ± SD. **, P<0.01; ***, P<0.001. hBMECs, human brain microvascular endothelial cells; RT-PCR, reverse transcription-polymerase chain reaction; NC, negative control; SD, standard deviation; HICH, hypertensive intracerebral hemorrhage; GAPDH, glyceraldehyde-3-phosphate dehydrogenase; ZO-1, zonula occludens 1; FITC, fluorescein isothiocyanate; MMP2, matrix metallopeptidase 2; TCF-4, transcription factor 4; LEF-1, lymphoid enhancer binding factor 1; IL-8, interleukin-8.

Effect of miR-145-5p/MMP2 axis in HICH rat model

The RT-PCR results revealed that the expression of miR-145-5p in the brain tissues of the rat HICH model was significantly decreased compared with the sham group. Moreover, and the expression of miR-145-5p was significantly increased in HICH + AAV-miR-145-5p group compared with the HICH + AAV-control group (*Figure 6A*). At 24, 48, 72 h after operation, the neurological function of rats was assessed using the mNSS and mLPT. The mNSS (*Figure 6B*) scores of the HICH and HICH + AAV-control groups were significantly higher than those of the sham group across all three time points. Compared with the rats in the HICH and HICH + AAV-control groups, the scores in the HICH + AAV-miR-145-5p group were significantly decreased but did not reach the level of the sham group. In contrast, the mLPT scores showed an opposite trend (*Figure 6C*). Brain water content was significantly higher in the HICH and HICH + AAV-control groups than in the sham group. Also, infusion of miR-145-5p significantly attenuated the increased brain water content in HICH animals (*Figure 6D*). Staining with H&E also confirmed that miR-145-5p attenuated brain edema after HICH (*Figure 6E*). TUNEL staining showed that miR-145-5p intervention could significantly reduce neuronal apoptosis after HICH (*Figure 6F*).

To evaluate the effect of miR-145-5p on endothelial tight junctions of the BBB after HICH, we examined the expression of ZO-1 and occludin using immunofluorescence. The number of ZO-1- and occludin-positive cells was significantly decreased in the HICH and HICH + AAV-control groups compared with the sham group, but the HICH + AAV-miR-145-5p group had significantly increased numbers of ZO-1- and occludin-positive cells relative to the HICH + AAV-control group (*Figure 7A*). Moreover, the expression of MMP2, Wnt3, β-catenin, TCF-4, LEF-1 and IL-8 in the HICH + AAV-miR-145-5p group was lower compared with the HICH and HICH + AAV-control groups (*Figure 7B*).

Discussion

Recent evidence has shown that better understanding of dysregulated miRNAs in the pathogenesis of HICH may help discover specific molecular targets for HICH treatment (22). Studies have shown that miR-145 is essential for differentiation of VSMCs and phenotypic transformation (13,14). In the rat model of spontaneous hypertension, the highly expressed long non-coding RNA (lncRNA)-TUGI acts as a "sponge" of miR-145 by competitively binding to miR-145 with FGF10, leading to upregulation of the expression of target gene *FCF10* and enhancing the proliferation and migration of VSMCs (15). Nevertheless, whether miR-145-5p is involved in regulating the function of HICH and further regulating the permeability of microvascular endothelial cells remains to be determined.

In the present study, we found that miR-145-5p was downregulated in both HIHC cell and rat models. The miR-145-5p overexpression contributed to suppressing vascular permeability and angiogenesis. The formation of cerebral edema after ICH is the most important pathological change and also the key factor leading to clinical deterioration (23). Our results revealed that miR-145-5p overexpression could reduce hemispheric water content, perihematomal neuronal death and cell apoptosis in HICH rats. Furthermore, overexpression of miR-145-5p also increased ZO-1 and occludin expressions in the perihematomal regions. Ultimately, this will significantly inhibit the apoptosis of brain tissues, reduce neuronal injury, and alleviate sequelae after HICH, such as cognitive and motor disorders.

Previous research has shown that miRNAs invariably exhibit regulatory activities in HICH damage by directly binding to the 3'-UTR of target mRNAs. By targeting VEGFA, miR-126 knockdown increased apoptosis in hBMECs (22). Using a luciferase reporter experiment, we identified MMP2 as a possible target of miR-145-5p and demonstrated how it might control MMP2 by directly binding to its 3'-UTR. MMP2 and many other MMP families play a vital role in the pathological process of BBB proteolytic degradation (19,24). In our study, MMP2 co-expressed negatively with miR-145-5p in thrombin-treated hBMECs, promoting ZO-1 and occludin expression, increasing vascular permeability, and activating angiogenesis. Additionally, MMP2 and the downstream Wnt/β-catenin signaling pathway are implicated in the neurological deficits associated with HICH. Our findings offer preliminary evidence that miR-145-5p modulates cell damage in HICH by inhibiting the Wnt/β-catenin pathway.

In conclusion, miR-145-5p can protect brain injury in HICH by inhibiting the MMP2-mediated Wnt/β-catenin signaling pathway, thus enhancing neural function, resolving BBB disruption, attenuating brain edema, and decreasing apoptosis. The current findings suggest new

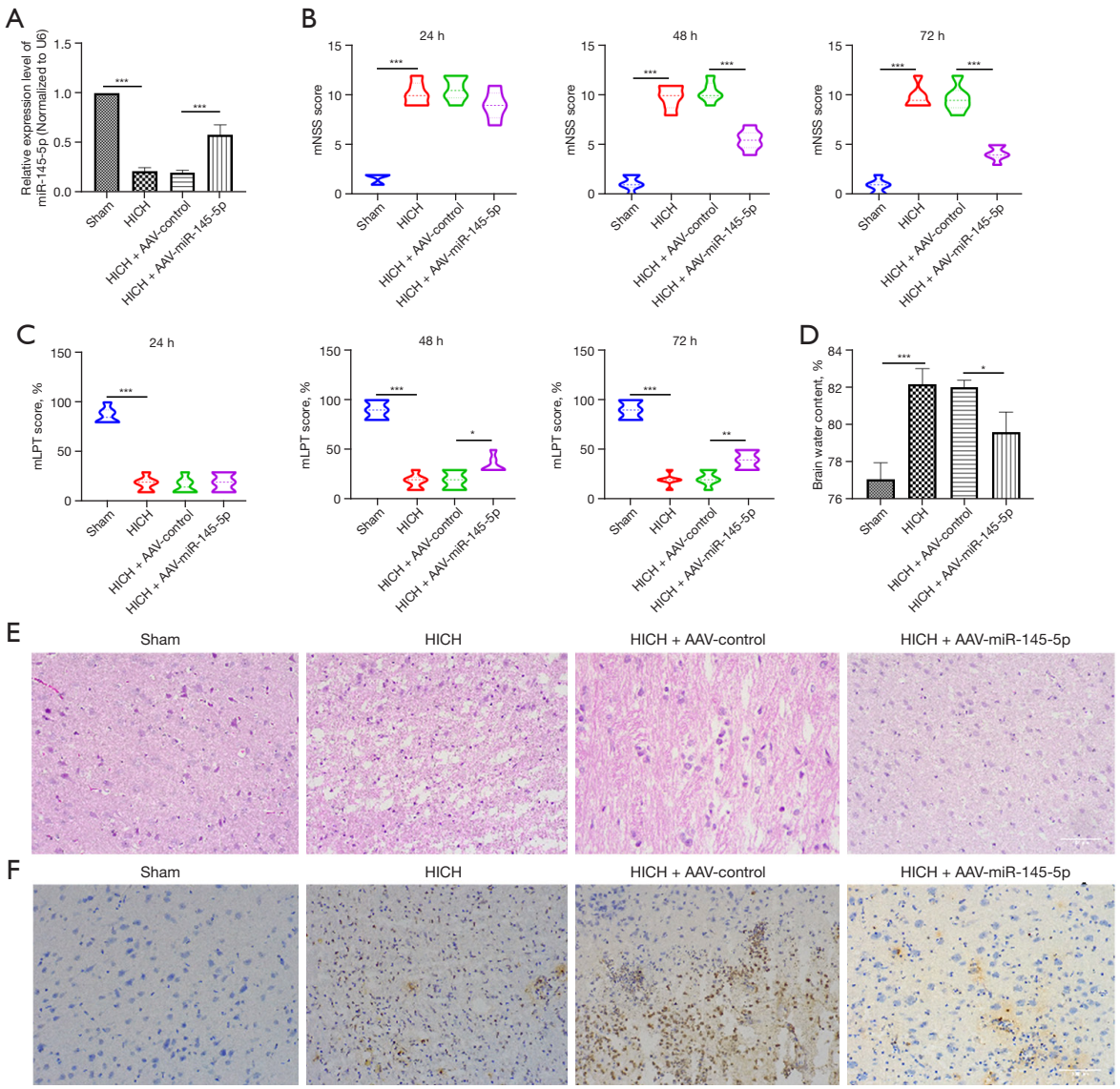

Figure 6 Effect of miR-145-5p in the HICH rat model. (A) Expression levels of miR-145-5p in brain tissues of HICH rats. (B,C) Functional outcomes (mNSS and mLPT) evaluated by independent blinded investigators at 24, 48, 72 h after operation. (D) Brain water content in different groups; (E) H&E staining (200× magnification, scale bar: 50 μm); (F) cell apoptosis determined by TUNEL assay (200× magnification, scale bar: 50 μm), TUNEL positive nuclei in red fluorescent color and total nuclei staining with DAPI. *, P<0.05; **, P<0.01; ***, P<0.001. HICH, hypertensive intracerebral hemorrhage; AAV, adeno-associated virus; mNSS, modified neurological severity score; mLPT, modified limb placing tests; DAPI, 4',6-diamidino-2-phenylindole dihydrochloride.

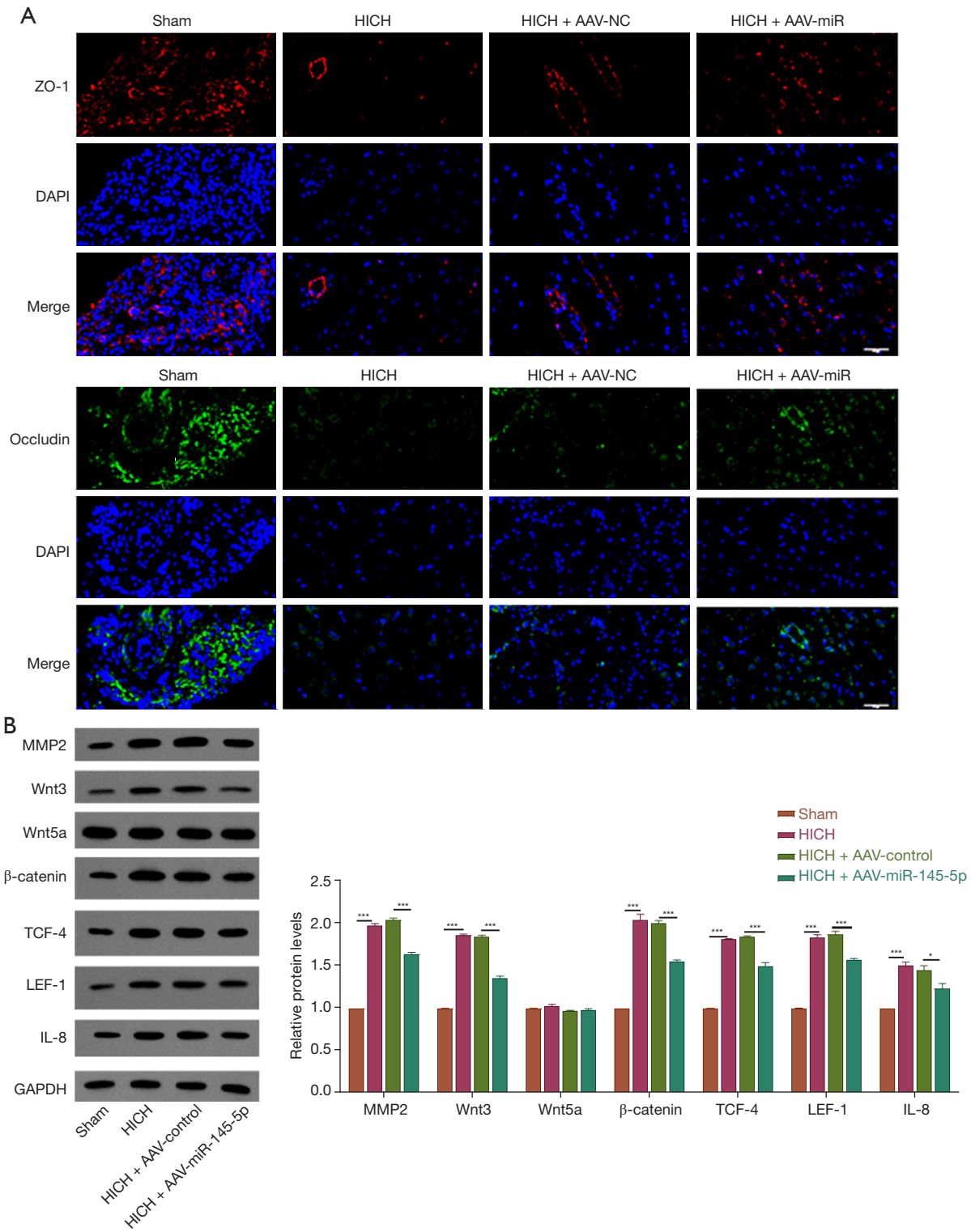

Figure 7 Effect of miR-145-5p in HICH rat model. (A) The protein expression levels of ZO-1 and occludin were determined by immunofluorescence (scale bar: 50 μm); (B) the protein levels of MMP2, Wnt3, Wnt5a, β-catenin, TCF-4, LEF-1 and IL-8 in different groups detected by western blot analysis. *, P<0.05; ***, P<0.001. HICH, hypertensive intracerebral hemorrhage; DAPI, 4',6-diamidino-2-phenylindole dihydrochloride.

therapeutic avenues for HICH and provide a theoretical foundation for better understanding the disease's etiology.

Acknowledgments

Funding: This study was supported by the Key Research Project of Science and Technology Department of Sichuan Province (grant/award No. 2017JY0035, to Wenfeng Xiao), Health Commission of Mianyang City (grant/award No. 202044) and Key Research and Development Project of Science and Technology Department of Sichuan Province (grant/award No. 2019YFS0392, to Jianguo Xu).

Footnote

Reporting Checklist: The authors have completed the ARRIVE reporting checklist. Available at https://atm.amegroups.com/article/view/10.21037/atm-22-1897/rc

Data Sharing Statement: Available at https://atm.amegroups.com/article/view/10.21037/atm-22-1897/dss

Conflicts of Interest: All authors have completed the ICMJE uniform disclosure form (available at https://atm.amegroups.com/article/view/10.21037/atm-22-1897/coif). The authors have no conflicts of interest to declare.

Ethical Statement: The authors are accountable for all aspects of the work in ensuring that questions related to the accuracy or integrity of any part of the work are appropriately investigated and resolved. The animal experiments were performed according to the National Institutes of Health's Guidelines for the Care and Use of Laboratory Animals and were granted approval by the Animal Care and Research Committee of West China Hospital of Sichuan University (No. 20211047A).

References

1. Qureshi AI, Qureshi MH. Acute hypertensive response in patients with intracerebral hemorrhage pathophysiology and treatment. J Cereb Blood Flow Metab 2018;38:1551-63.
2. Lee KR, Kawai N, Kim S, et al. Mechanisms of edema formation after intracerebral hemorrhage: effects of thrombin on cerebral blood flow, blood-brain barrier permeability, and cell survival in a rat model. J Neurosurg 1997;86:272-8.
3. Reznik ME, Fakhri N, Moody S, et al. Arrival blood pressure in hypertensive and non-hypertensive spontaneous intracerebral hemorrhage. J Neurol Sci 2020;416:117000.
4. Ma H, Guo ZN, Sun X, et al. Hematoma volume is a predictive factor of disturbed autoregulation after spontaneous intracerebral hemorrhage. J Neurol Sci 2017;382:96-100.
5. Kidwell CS, Rosand J, Norato G, et al. Ischemic lesions, blood pressure dysregulation, and poor outcomes in intracerebral hemorrhage. Neurology 2017;88:782-8.
6. Hammond SM. An overview of microRNAs. Adv Drug Deliv Rev 2015;87:3-14.
7. Fabian MR, Sonenberg N, Filipowicz W. Regulation of mRNA translation and stability by microRNAs. Annu Rev Biochem 2010;79:351-79.
8. O'Brien J, Hayder H, Zayed Y, et al. Overview of MicroRNA Biogenesis, Mechanisms of Actions, and Circulation. Front Endocrinol (Lausanne) 2018;9:402.
9. Yi X, Tang X. Exosomes From miR-19b-3p-Modified ADSCs Inhibit Ferroptosis in Intracerebral Hemorrhage Mice. Front Cell Dev Biol 2021;9:661317.
10. Wei M, Li C, Yan Z, et al. Activated Microglia Exosomes Mediated miR-383-3p Promotes Neuronal Necroptosis Through Inhibiting ATF4 Expression in Intracerebral Hemorrhage. Neurochem Res 2021;46:1337-49.
11. Wang X, Hong Y, Wu L, et al. Deletion of MicroRNA-144/451 Cluster Aggravated Brain Injury in Intracerebral Hemorrhage Mice by Targeting 14-3-3ζ. Front Neurol 2021;11:551411.
12. Cheng X, Ander BP, Jickling GC, et al. MicroRNA and their target mRNAs change expression in whole blood of patients after intracerebral hemorrhage. J Cereb Blood Flow Metab 2020;40:775-86.
13. Wang YS, Li SH, Guo J, et al. Role of miR-145 in cardiac myofibroblast differentiation. J Mol Cell Cardiol

2014;66:94-105.
14. Xu J, Yan S, Tan H, et al. The miR-143/145 cluster reverses the regulation effect of KLF5 in smooth muscle cells with proliferation and contractility in intracranial aneurysm. Gene 2018;679:266-73.
15. Shi L, Tian C, Sun L, et al. The lncRNA TUG1/miR-145-5p/FGF10 regulates proliferation and migration in VSMCs of hypertension. Biochem Biophys Res Commun 2018;501:688-95.
16. Liao J, Zhang Y, Wu Y, et al. Akt modulation by miR-145 during exercise-induced VSMC phenotypic switching in hypertension. Life Sci 2018;199:71-9.
17. Ren L, Wei C, Li K, et al. miR-145LncRNA MALAT1 up-regulates VEGF-A and ANGPT2 to promote angiogenesis in brain microvascular endothelial cells against oxygen-glucose deprivation via targetting. Biosci Rep 2019;39:BSR20180226.
18. Li LL, Mao CD, Wang GP, et al. MiR-145-5p alleviates hypoxia/reoxygenation- induced cardiac microvascular endothelial cell injury in coronary heart disease by inhibiting Smad4 expression. Eur Rev Med Pharmacol Sci 2020;24:5008-17.
19. Hernandez-Guillamon M, Martinez-Saez E, Delgado P, et al. MMP-2/MMP-9 plasma level and brain expression in cerebral amyloid angiopathy-associated hemorrhagic stroke. Brain Pathol 2012;22:133-41.
20. Sansing LH, Kaznatcheeva EA, Perkins CJ, et al. Edema after intracerebral hemorrhage: correlations with coagulation parameters and treatment. J Neurosurg 2003;98:985-92.
21. Zhou L, Deng L, Chang NB, et al. Cell apoptosis and proliferation in rat brains after intracerebral hemorrhage: role of Wnt/beta-catenin signaling pathway. Turk J Med Sci 2014;44:920-7.
22. Dong B, Zhou B, Sun Z, et al. LncRNA-FENDRR mediates VEGFA to promote the apoptosis of brain microvascular endothelial cells via regulating miR-126 in mice with hypertensive intracerebral hemorrhage. Microcirculation 2018;25:e12499.
23. Gebel JM, Brott TG, Sila CA, et al. Decreased perihematomal edema in thrombolysis-related intracerebral hemorrhage compared with spontaneous intracerebral hemorrhage. Stroke 2000;31:596-600.
24. Katsu M, Niizuma K, Yoshioka H, et al. Hemoglobin-induced oxidative stress contributes to matrix metalloproteinase activation and blood-brain barrier dysfunction in vivo. J Cereb Blood Flow Metab 2010;30:1939-50.

(English Language Editor: K. Brown)

Cite this article as: Xiao W, Jiang Z, Wan W, Pan W, Xu J. miR-145-5p targets MMP2 to protect brain injury in hypertensive intracerebral hemorrhage via inactivation of the Wnt/β-catenin signaling pathway. Ann Transl Med 2022;10(10):571. doi: 10.21037/atm-22-1897

